PHYSICAL REVIEW A **71**, 060303(R) (2005)

High-fidelity *Z*-measurement error encoding of optical qubits

J. L. O'Brien, G. J. Pryde, A. G. White, and T. C. Ralph
Centre for Quantum Computer Technology, Department of Physics, University of Queensland, 4072, Australia
(Received 9 August 2004; published 9 June 2005)

We demonstrate a quantum error correction scheme that protects against accidental measurement, using a parity encoding where the logical state of a single qubit is encoded into two physical qubits using a nondeterministic photonic controlled-NOT gate. For the single qubit input states $|0\rangle$, $|1\rangle$, $|0\rangle \pm |1\rangle$, and $|0\rangle \pm i|1\rangle$ our encoder produces the appropriate two-qubit encoded state with an average fidelity of 0.88 ± 0.03 and the single qubit decoded states have an average fidelity of 0.93 ± 0.05 with the original state. We are able to decode the two-qubit state (up to a bit flip) by performing a measurement on one of the qubits in the logical basis; we find that the 64 one-qubit decoded states arising from 16 real and imaginary single-qubit superposition inputs have an average fidelity of 0.96 ± 0.03.

DOI: 10.1103/PhysRevA.71.060303 PACS number(s): 03.67.Lx, 03.67.Pp, 42.50.Dv

One of the greatest promises of quantum information science is the exponential improvement in the computational power offered by a quantum computer for certain tasks [1]. Experimental progress has been made in NMR [2], ion trap [3,4], cavity QED [5], superconducting [6], and spin [7] qubits. A relatively recent proposal by Knill, Laflamme, and Milburn (KLM) is linear optics quantum computing (LOQC) [8] in which quantum information is encoded in single photons, and the nonlinear interaction required for two photon gates is realized through conditional measurement [9–12]. The critical challenge for all architectures is achieving fault tolerance; this will require quantum error correction (QEC) [13,14]: a logical qubit $|\psi\rangle_L$ is encoded in a number of physical qubits such that joint measurements of the qubits can extract information about errors without destroying the quantum information. A five-qubit encoding against all one-qubit errors has been demonstrated in NMR [15]. A two-qubit encoding, $\alpha|00\rangle + \beta|11\rangle$, has been demonstrated with polarization single photon qubits [16].

A simple QEC code is the one introduced by KLM that protects against a computational basis measurement—*Z measurement*—of one of the qubits [8]

$$|\psi\rangle_L = \alpha|0\rangle_L + \beta|1\rangle_L = \alpha(|00\rangle + |11\rangle) + \beta(|01\rangle + |10\rangle). \tag{1}$$

This is a parity encoding: $|0\rangle_L$ is represented by all even parity combinations of the two qubits; $|1\rangle_L$ by all the odd parity combinations. If a *Z* measurement is made on either of the physical qubits and the result "0" is obtained, then the state collapses to an unencoded qubit, but the superposition is preserved; if the result is "1" a bit-flipped version of the unencoded qubit is the result. This generalizes straightforwardly to an *n*-qubit code [17]: if a *Z* measurement occurs on any of the qubits, the encoding is simply reduced to $n-1$ qubits. This type of QEC is critical for a scale up of LOQC circuits: KLM showed that their nondeterministic, teleported controlled-NOT (CNOT) gate [8] fails by performing a *Z* measurement on one of the qubits (this is also true for equivalent gates [18,19]). Thus by using this QEC technique the qubits can be protected against gate failures and so the effective success rate of gate operations can be boosted. A similar principle underlies alternative LOQC schemes [20,21] in which a quantum computation proceeds by generating a highly entangled state of many qubits—a cluster state—and then performing only single qubit measurements in a basis determined from the outcome of previous measurements [22]. Like the *n*-qubit *Z*-error QEC code, these cluster states are robust against accidental *Z* measurement. The encoding of Eq. (1) also forms the basic element in a redundancy code, which can be used to correct for photon loss errors [23]: $|\psi\rangle_{LL} = \alpha|0\rangle_L|0\rangle_L + \beta|1\rangle_L|1\rangle_L$. For these reasons it is important to show that qubit states can be encoded with high fidelity and recovered with high fidelity after *Z* measurements.

Here we report an experimental demonstration of QEC using the two-qubit code of Eq. (1), in which the encoded state is prepared from an arbitrary input state, the error is induced, and syndrome measured. The final bit flip correction is not made. A single qubit prepared in an arbitrary state $|\psi\rangle = \alpha|0\rangle + \beta|1\rangle$ is input into the target mode of a nondeterministic photonic CNOT gate. An ancilla qubit in the real equal superposition $|0\rangle + |1\rangle$ is input into the control. We use quantum state tomography to determine the resulting two-qubit encoded state generated for the inputs $|\psi\rangle = |0\rangle, |1\rangle, |0\rangle \pm |1\rangle$, and $|0\rangle \pm i|1\rangle$ (neglecting normalization), and find an average fidelity of $F = 0.88 \pm 0.03$ with $|\psi\rangle_L$. For the same six one-qubit inputs, the average fidelity of the reconstructed one-qubit decoded states is $F = 0.93 \pm 0.05$. Finally, we test the decoding (and encoding) by measuring one or other of the qubits in the computational basis for 16 different real and imaginary superposition inputs and performing one-qubit quantum state tomography on the second qubit. We find that the average fidelity of this second qubit with the state $|\psi\rangle = \alpha|0\rangle + \beta|1\rangle$ or the bit-flipped version of it $|\psi'\rangle = \beta|0\rangle + \alpha|1\rangle$ is $F = 0.96 \pm 0.03$. These results demonstrate that high fidelity *Z*-measurement QEC is possible for a simple two-qubit code.

Figure 1(a) shows schematically how the encoding of Eq. (1) can be achieved using a CNOT gate and an ancilla qubit prepared in the state $|0\rangle + |1\rangle$. Figure 1(a) also shows how a projective measurement of one of the qubits in the logical basis, plus a bit-flip *X* operation, conditional on the measure-

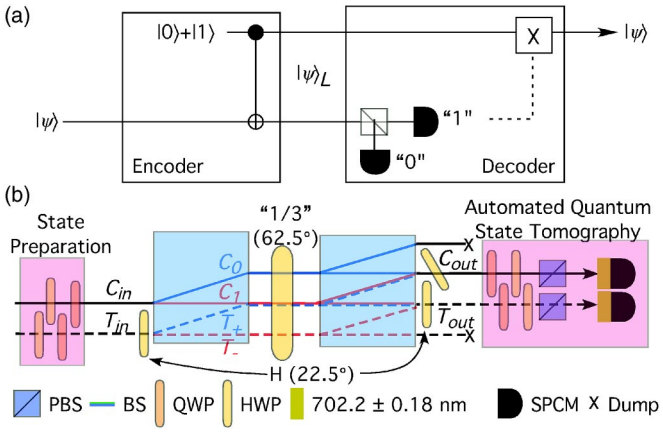

FIG. 1. Encoding against *Z*-measurement error. (a) A schematic of a circuit for performing the encoding and decoding of the state $|\psi\rangle_L$. The circuit consisits of a CNOT gate with the control input set to $|0\rangle+|1\rangle$ and the arbitrary, one-qubit state to be encoded $|\psi\rangle$ input into the target. Note that decoding can be achieved by measuring either of the encoded qubits. (b) Schematic of the experimental CNOT gate shown in (a), as originally demonstrated in [10].

ment outcome, acts as a decoder. The CNOT gate used in our demonstration is shown schematically in Fig. 1(b). It operates nondeterministically and successful events are postselected by coincidence measurements. For a detailed description of its operation see Ref. [10]. Pairs of energy degenerate nonentangled photons of wavelength $\lambda=702.2$ nm were generated in a nonlinear β-barium-borate (BBO) crystal through spontaneous parametric down conversion of a $\lambda=351.1$ nm, $P\approx 900$ mW pump beam. A coincidence window of 1 ns was used and no correction for accidental counts was made. These photons were sent through a polarizing beam splitter (PBS) to prepare a highly pure horizontal polarization state. Qubits are stored in the polarization state of these two photons using the assignment: horizontal $|H\rangle\equiv|0\rangle$; and vertical $|V\rangle\equiv|1\rangle$. The control input is prepared in the equal real superposition $|0\rangle+|1\rangle$ using a half wave plate (HWP) with its optic axis at 22.5°. An arbitrary $|\psi\rangle$ was prepared using a HWP and quarter wave plate (QWP). The output of the circuit, nominally $|\psi\rangle_L$, was analyzed using standard two-qubit quantum state tomography [24]. The required two-qubit measurements [24] were performed using a pair of analyzers each consisting of a QWP and HWP followed by a PBS and a single photon counting module. Each analyzer can perform any one-qubit projective measurement.

We firstly confirm that this circuit produces the correct two-qubit encoded state: Table I shows six one-qubit inputs (the two eigenstates and four equal superpositions) and the corresponding ideal encoded states. For these six one-qubit input states we used our encoding circuit to produce a two-qubit encoded state and performed two-qubit quantum state tomography on the output. The real and imaginary parts of the density matrices for the six two-qubit encoded states are shown in Fig. 2. These experimentally measured encoded states have an average fidelity of $F=0.88\pm0.03$ with $|\psi\rangle_L$ (where the error bar is the standard deviation), demonstrating the high fidelity of the encoding operation.

Next we test how well the encoding has worked by assuming the capability to perform perfect decoding and so

TABLE I. One-qubit input states and the ideal corresponding two-qubit encoded states.

1-qubit input $\lvert\psi\rangle=\alpha\lvert0\rangle+\beta\lvert1\rangle$	2-qubit encoded state $\lvert\Psi\rangle=\alpha\lvert00\rangle+\beta\lvert01\rangle+\beta\lvert10\rangle+\alpha\lvert11\rangle$	Fig. 2
$\lvert0\rangle$	$\lvert00\rangle+\lvert11\rangle$	2(a)
$\lvert1\rangle$	$\lvert01\rangle+\lvert10\rangle$	2(d)
$\lvert0\rangle+\lvert1\rangle$	$\lvert00\rangle+\lvert01\rangle+\lvert10\rangle+\lvert11\rangle$	2(b)
$\lvert0\rangle-\lvert1\rangle$	$\lvert00\rangle-\lvert01\rangle-\lvert10\rangle+\lvert11\rangle$	2(e)
$\lvert0\rangle+i\lvert1\rangle$	$\lvert00\rangle+i\lvert01\rangle+i\lvert10\rangle+\lvert11\rangle$	2(c)
$\lvert0\rangle-i\lvert1\rangle$	$\lvert00\rangle-i\lvert01\rangle-i\lvert10\rangle+\lvert11\rangle$	2(f)

theoretically extract the one-qubit decoded states from the two-qubit encoded states shown in Fig. 2. The one-qubit decoded state can be produced in four ways: by measuring either the first or second qubit in the computational basis, and getting the result "0" or "1." In Fig. 3 we show all four reconstructed one-qubit density matrices extracted from each of the six encoded states in Fig. 2. We show the imaginary components only for the imaginary superpositions since in all other cases these components should be zero, and are measured to be relatively small (the average of imaginary components is 0.04 ± 0.04). The average fidelity of these one-

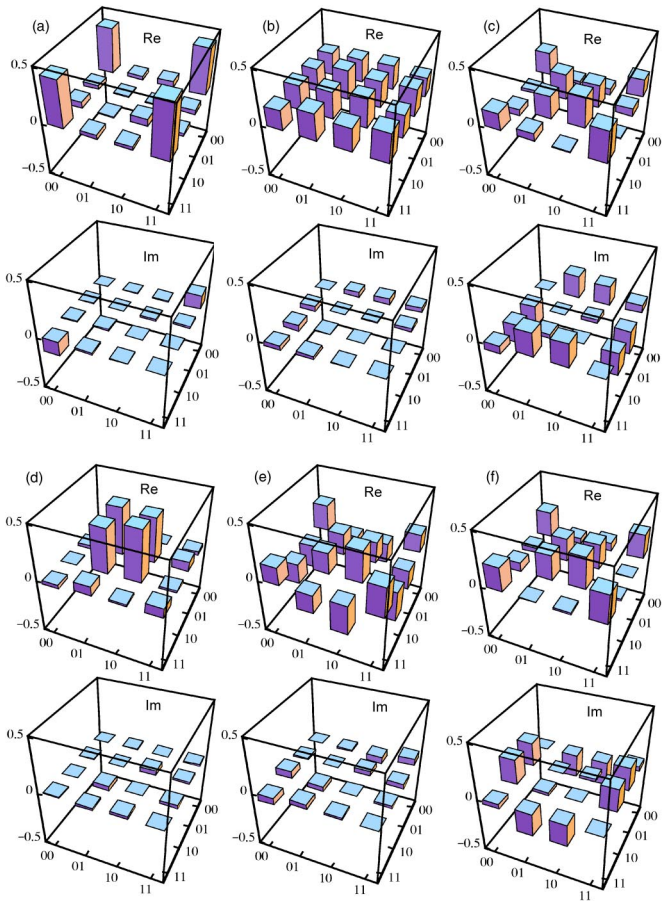

FIG. 2. Two-qubit encoded states. The real and imaginary parts of the density matrices are shown for the encoded states produced for the one-qubit inputs given in Table I.

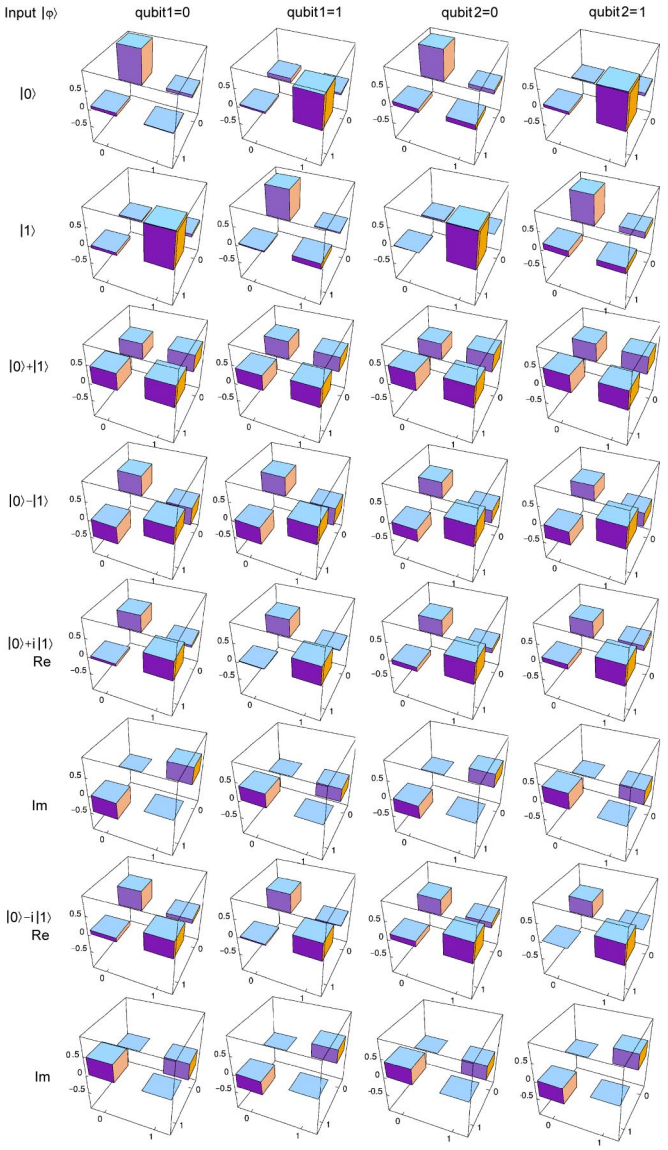

FIG. 3. One-qubit decoded states. A table of density matrices for the six inputs and four decoding measurements listed in the figure. The imaginary parts are shown for the $|0\rangle+i|1\rangle$ and $|0\rangle-i|1\rangle$ inputs only.

qubit states with $|\psi\rangle$ or $|\psi'\rangle$ is $F=0.93\pm0.05$. Since these states are reconstructed from the six two-qubit states, this result demonstrates that given perfect decoding, the one-qubit decoded states are more robust to imperfections in the encoder than the two-qubit encoded states.

Finally we test the decoding circuit (as well as the encoding circuit) by preparing the one-qubit input in the unequal amplitude, real superpositions $\cos(\theta)|0\rangle+\sin(\theta)|1\rangle$, and equal amplitude, variable phase superpositions $|0\rangle+e^{i(90°-2\phi)}|1\rangle$, for θ, $\phi=10°$, 20°, 30°, 40°, 50°, 60°, 70°, and 80°. Together with the results of Fig. 3 (giving θ, $\phi=0°$ and 90°), these states map out two orthogonal great semicircles on the Bloch sphere. For each of these inputs we reconstructed the one-qubit density matrix *directly* for both measurement outcomes on both qubits, i.e., four one-qubit density matrices for each input state. From these density matrices we calculated the

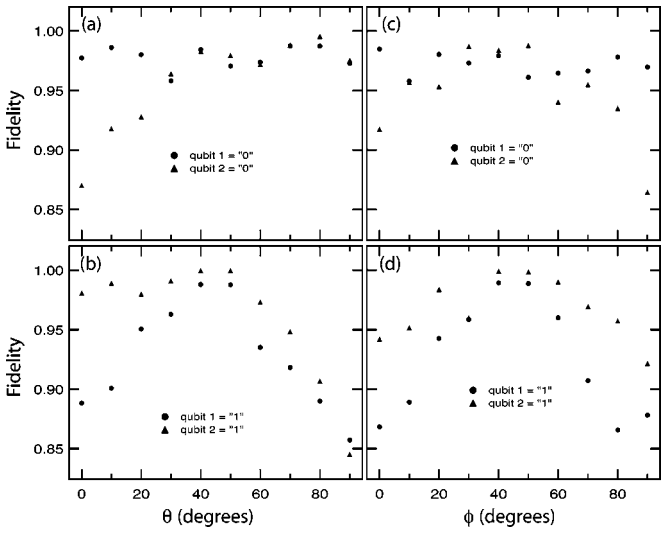

FIG. 4. One-qubit decoded state fidelities for the one-qubit input states $\cos(\theta)|0\rangle+\sin(\theta)|1\rangle$ and $|0\rangle+e^{i(90°-2\phi)}|1\rangle$.

fidelity with the ideal state $|\psi\rangle$ or $|\psi'\rangle$. The results are shown in Fig. 4. The average fidelity for all of these states (excluding θ, $\phi=0°$ and 90°) is 0.96 ± 0.03, which is the same, to within error, as for the reconstructed states shown in Fig. 3.

The behavior observed in Fig. 4 can be explained in terms of the classical and nonclassical interference requirements of the CNOT gate: The gate splits and recombines the control and target polarization modes requiring two classical interferences, and nonclassically interferes the control $|V\rangle$ and target $|H\rangle-|V\rangle$ modes [10]. In practice, the visibility of each of these interferences is subunity and thus contributes to errors in the operation of the gate: The encoder works well for $\theta=\phi=45°$, i.e., the input state $|0\rangle+|1\rangle(=|H\rangle+|V\rangle)$ since no nonclassical interference is required, and only one classical interference is required for the control. The encoder also works well when qubit 1 (the output of the control mode) is measured to be $|0\rangle$ since, again, only one classical interference is required. Finally, the encoder works well for θ close to zero, which is expected from Fig. 2(a), which shows that the $|01\rangle\langle01|$ population, the main contributor to errors in this case, is very small.

This two-qubit *Z*-error encoding could be extended to a *n*-qubit encoding using additional CNOT gates with single photons prepared in the $|0\rangle+|1\rangle$ state as the control input, and any of the already encoded qubits as the target. A very similar technique can be used to build up a cluster state using controlled-phase (CZ) gates [20]. Note, however, that our CNOT gate succeeds with the probability of 1/9 [25], but can in principle be made deterministic and scalable [10]. In order to build up the parity encoding or a cluster state in a scalable way teleportation gates or similar techniques [21] would be needed.

In conclusion, we have experimentally demonstrated a high fidelity realisation of a two-qubit *Z*-measurement QEC scheme (up to implementation of an *X* gate). For a representative set of input states the average fidelity of the one-qubit decoded state is 0.96 ± 0.03. Our scheme uses a nondetermin-

istic CNOT gate operating on the polarization states of single photon qubits, and is therefore a nondeterministic encoding and will not be useful in its own right for a scalable quantum computer. However, this does provide a proof of principle of an encoding against a realistic error in linear optics quantum computing. The technique can be extended to a larger encoded state or to the creation of a cluster state by using CZ gates.

This work was supported by the Australian Research Council, the NSA and ARDA under ARO Contract No. DAAD 19-01-1-0651.

[1] M. A. Nielsen and I. L. Chuang, *Quantum Computation and Quantum Information* (Cambridge University Press, Cambridge, 2000), p. 91.
[2] L. M. K. Vandersypen, M. Steffen, G. Breyta, C. S. Yannoni, M. H. Sherwood, and I. L. Chuang, Nature (London) **414**, 883 (2001).
[3] F. Schmidt-Kaler, H. Häffner, M. Riebe, S. Gulde, G. P. T. Lancaster, T. Deuschle, C. Becher, C. F. Roos, J. Eschner, and R. Blatt, Nature (London) **422**, 408 (2003).
[4] D. Leibfried *et al.*, Nature (London) **422**, 412 (2003).
[5] Q. A. Turchette, C. J. Hood, W. Lange, H. Mabuchi, and H. J. Kimble, Phys. Rev. Lett. **75**, 4710 (1995).
[6] T. Yamamoto, Yu. A. Pashkin, O. Astafiev, Y. Nakamura, and J. S. Tsai, Nature (London) **425**, 941 (2003).
[7] R. G. Clark *et al.*, Philos. Trans. R. Soc. London **361**, 1451 (2003).
[8] E. Knill, R. Laflamme, and G. J. Milburn, Nature (London) **409**, 46 (2001).
[9] T. B. Pittman, M. J. Fitch, B. C. Jacobs, and J. D. Franson, Phys. Rev. A **68**, 032316 (2003).
[10] J. L. O'Brien, G. J. Pryde, A. G. White, T. C. Ralph, and D. Branning, Nature (London) **426**, 264 (2003); J. L. O'Brien, G. J. Pryde, A. Gilchrist, D. F. V. James, N. K. Langford, T. C. Ralph, and A. G. White, Phys. Rev. Lett. **93**, 080502 (2004).
[11] S. Gasparoni, J.-W. Pan, P. Walther, T. Rudolph, and A. Zeilinger, Phys. Rev. Lett. **93**, 020504 (2004).
[12] Z. Zhao, A.-N. Zhang, Y.-A. Chen, H. Zhang, J.-F. Du, T. Yang, and J.-W. Pan, Phys. Rev. Lett. **94**, 030501 (2005).
[13] P. W. Shor, Phys. Rev. A **52**, R2493 (1995).
[14] A. M. Steane, Phys. Rev. Lett. **77**, 793 (1996).
[15] E. Knill, R. Laflamme, R. Martinez, and C. Negrevergne, Phys. Rev. Lett. **86**, 5811 (2001).
[16] T. B. Pittman, B. C Jacobs, and J. D. Franson, Phys. Rev. A **69**, 042306 (2004).
[17] A. J. F. Hayes, A. Gilchrist, C. R. Myers, and T. C. Ralph, J. Opt. B: Quantum Semiclass. Opt. **6**, 533 (2004).
[18] T. B. Pittman, B. C. Jacobs, and J. D. Franson, Phys. Rev. A **64**, 062311 (2001).
[19] M. Koashi, T. Yamamoto, and N. Imoto, Phys. Rev. A **63**, 030301(R) (2001).
[20] M. A. Nielsen, Phys. Rev. Lett. **93**, 040503 (2004).
[21] D. E. Browne and T. Rudolph, e-print quant-ph/0405157.
[22] R. Raussendorf and H. J. Briegel, Phys. Rev. Lett. **86**, 5188 (2001).
[23] T. C. Ralph, A. J. F. Hayes, and A. Gilchrist, e-print quant-ph/0501184.
[24] D. F. V. James, P. G. Kwiat, W. J. Munro, and A. G. White, Phys. Rev. A **64**, 052312 (2001).
[25] T. C. Ralph, N. K. Langford, T. B. Bell, and A. G. White, Phys. Rev. A **65**, 062324 (2001).